High-Brightness and Low-Voltage Light-Emitting Devices Based on Trischelated Ruthenium(II) and Tris(2,2′-bipyridine)osmium(II) Emitter Layers and Low Melting Point Alloy Cathode Contacts

Frank G. Gao[†] and Allen J. Bard[*],[‡]

Department of Chemistry & Biochemistry, The University of Texas at Austin, Austin, Texas 78712, and Wyle Laboratories, Mail Code BT-37, 1290 Hercules Drive, Suite 120, Houston, Texas 77058

Solid-state light-emitting devices (LEDs) were fabricated based on an amorphous film of $Ru(bpy)_3(ClO_4)_2$ (bpy = 2,2′-bipyridine) about 100 nm thick on indium−tin oxide (ITO) with printed low melting point alloys, such as Ga:In, Ga:Sn, and Bi:In:Pb:Sn, as cathodic contacts. A device with the structure of ITO ($\leq$10 Ω/square)/$Ru(bpy)_3(ClO_4)_2$/Ga:Sn produces a bright red emission (3500 cd/m^2 at 4.0 V) centered at 660 nm. This new method of making contacts significantly simplifies the fabrication of an electroluminescence cell and has potential application in the production of LEDs by inkjet or microcontact printing. LEDs based on C_{12}−$Ru(bpy)_3(ClO_4)_2$, $Ru(phenanthroline)_3(ClO_4)_2$, and $Os(bpy)_3(PF_6)_2$ were also studied. Low melting point alloy contacts were also used with cells based on tris(8-hydroxyquinoline)-aluminum.

Organic solid-state light-emitting devices (OLEDs) may eventually offer an alternative to inorganic semi-conductor (e.g., GaAs) light-emitting diodes and liquid crystal displays, perhaps affording flatter, brighter, and more flexible displays at lower cost.[1−5] There has been a great deal of research aimed at the development of new light-emitting materials.[6−19] Among the materials that have been studied, polymers based on trischelated

ruthenium(II) complexes have recently attracted con-siderable attention.[20−26] Attempts have been made to increase the duration of operation and to improve the performance of light-emitting materials with dopant in the emitters,[27−30] dopant in the hole-transport mater-ials,[31−34] electron-transport materials,[35,36] transparent

---

* To whom correspondence should be addressed. Tel: (512) 471-3761. Fax: (512) 471-0088. E-mail: ajbard@mail.utexas.edu.
† Wyle Laboratories. Tel: (281) 483-5290 (office) and (281) 483-7299 (lab). Fax: (281) 483-0402. E-mail: fgao@ems.jsc.nasa.gov.
‡ The University of Texas at Austin.

(1) Tang, C. W.; Vanslyke, S. A. *Appl. Phys. Lett.* **1987,** *51,* 913.
(2) Burroughes, J. H.; Bradley, D. D. C.; Brown, A. R.; Marks, R. N.; Mackay, K.; Friend, R. H.; Burns, P. L.; Holmes, A. B. *Nature* **1990,** *347,* 539.
(3) Sheats, J. R.; Antoniadis, H.; Hueschen, M.; Leonard, W.; Miller, J.; Moon, R.; Roitman, D.; Stocking, A. *Science* **1996,** *273,* 884.
(4) Sheats, J. R.; Chang, Y.; Roitman, D. B.; Stocking, A. *Acc. Chem. Res.* **1999,** *32,* 193.
(5) Forrest, S. R. *Chem. Rev.* **1997,** *97,* 1793.
(6) Yang, J. P.; Heremans, P. L.; Hoefnagels, R.; Tachelet, W.; Dieltiens, P.; Blockhuys, F.; Geise, H. J.; Borghs, G. *Synth. Met.* **2000,** *108,* 95.
(7) He, Y.; Kanick, J. *Appl. Phys. Lett.* **2000,** *76,* 661.
(8) Baldo, M. A.; Lamansky, S.; Burrows, P. E.; Thompson, M. E.; Forrest, S. R. *Appl. Phys. Lett.* **1999,** *75,* 4.
(9) O'Brien, D. F.; Baldo, M. A.; Thompson, M. E.; Forrest, S. R. *Appl. Phys. Lett.* **1999,** *74,* 442.
(10) Tao, X. T.; Suzuki, H.; Wada, T.; Miyata, S.; Sasabe, H. *J. Am. Chem. Soc.* **1999,** *121,* 9447.
(11) Gigli, G.; Barbarella, G.; Favaretto, L.; Cacialli, F.; Cingolani, R. *Appl. Phys. Lett.* **1999,** *75,* 439.
(12) Berkovich, E.; Klein, J.; Sheradsky, T.; Silcoff, E. R.; Ranjit, K. T.; Willner, I.; Nakhmanovich, G.; Gorelik, V.; Eichen, Y. *Synth. Met.* **1999,** *107,* 85.
(13) Curry, R. J.; Gillin, W. P. *Appl. Phys. Lett.* **1999,** *75,* 1380.
(14) Xu, C.; Cui, Y.; Shen, Y.; Gu, H.; Pan, Y.; Li, Y. *Appl. Phys. Lett.* **1999,** *75,* 1827.
(15) Curry, R. J.; Gillin, W. P. *Appl. Phys. Lett.* **1999,** *75,* 1380.
(16) Antoniadis, H.; Inbasekaran, M.; Woo, E. P. *Appl. Phys. Lett.* **1998,** *73,* 3055.
(17) Hamada, Y.; Kanno, H.; Sano, T.; Fujii, H.; Nishio, Y.; Takahashi, H.; Usuki, T.; Shibata, K. *Appl. Phys. Lett.* **1998,** *72,* 1939.
(18) Hamada, Y.; Sano, T.; Fujii, H.; Nishio, Y.; Takahashi, H.; Shibata, K. *Appl. Phys. Lett.* **1997,** *71,* 3338.
(19) Boyd, T. J.; Geerts, Y.; Lee, J.; Fogg, D. E.; Lavoie, G. G.; Schrock, R. R.; Rubner, M. F. *Macromolecules* **1997,** *30,* 3553.
(20) Maness, K. M.; Terrill, R. H.; Meyer, T. J.; Murray, R. W.; Wightman, R. M. *J. Am. Chem. Soc.* **1996,** *118,* 10609.
(21) Maness, K. M.; Masui, H.; Wightman, R. M.; Murray, R. W. *J. Am. Chem. Soc.* **1997,** *119,* 3987.
(22) Lyons, C. H.; Abbas, E. D.; Lee, J.-K.; Rubner, M. F. *J. Am. Chem. Soc.* **1998,** *120,* 12100.
(23) Handy, E. S.; Pal, A. J.; Rubner, M. F. *J. Am. Chem. Soc.* **1999,** *121,* 3525.
(24) Wu, A.; Yoo, D.; Lee, J.-K.; Rubner, M. F. *J. Am. Chem. Soc.* **1999,** *121,* 4883.
(25) Elliott, C. M.; Pichot, F.; Bloom, C. J.; Rider, L. S. *J. Am. Chem. Soc.* **1998,** *120,* 6781.
(26) Rubinstein, I.; Bard, A. J. *J. Am. Chem. Soc.* **1981,** *103,* 5007.
(27) Hamada, Y.; Kanno, H.; Tsuyoshi, T.; Takahashi, H.; Usuki, T. *Appl. Phys. Lett.* **1999,** *75,* 1682.
(28) Sakamoto, G.; Adachi, C.; Koyama, T.; Taniguchi, Y.; Merritt, C. D.; Murata, H.; Kafafi, Z. H. *Appl. Phys. Lett.* **1999,** *75,* 766.
(29) Kido, J.; Hongawa, K.; Okuyama, K.; Nagai, K. *Appl. Phys. Lett.* **1994,** *64,* 815.
(30) Sato, Y.; Ogata, T.; Ichinosawa, S.; Murata, Y. *Synth. Met.* **1997,** *91,* 103.
(31) Hu, N.; Xie, S.; Popovic, Z.; Ong, B.; Hor, A. *J. Am. Chem. Soc.* **1999,** *121,* 5097.
(32) Chung, J.; Choi, B.; Lee, H. H. *Appl. Phys. Lett.* **1999,** *74,* 3645.
(33) Blochwitz, J.; Pfeiffer, M.; Fritz, T.; Leo, K. *Appl. Phys. Lett.* **1998,** *73,* 729.
(34) Yamamori, A.; Adachi, C.; Koyama, T.; Taniguchi, Y. *Appl. Phys. Lett.* **1998,** *72,* 2147.
(35) Donze, N.; Pechy, P.; Gratzel, M.; Schaer, M.; Zuppiroli, L. *Chem. Phys. Lett.* **1999,** *315,* 405.
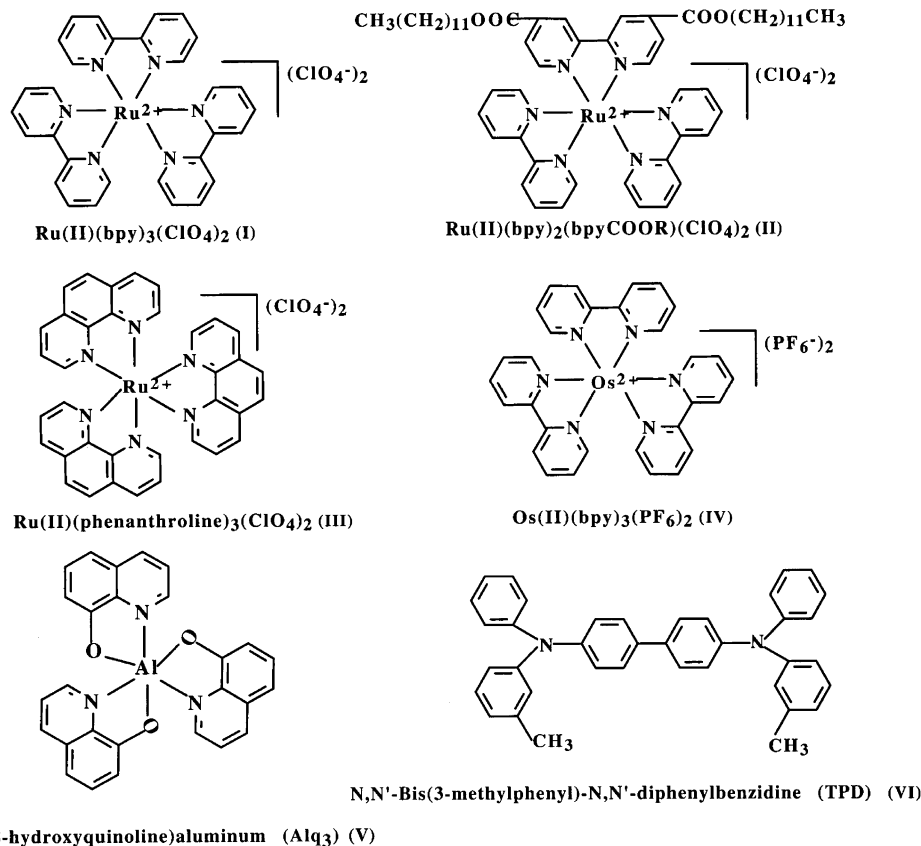(36) Jandke, M.; Strohriegl, P.; Berleb, S.; Werner, E.; Brutting, W. *Macromolecules* **1998,** *31,* 6434.

Figure 1. Chemical structures of the major compounds.

electrodes,[37] and surface treatment of indium−tin oxide (ITO).[38,39] Furthermore, with the realization that the overall improvement of the performance and durability of LEDs is related to the improvement of the metal contact, much research has been focused on understanding the nature of charge injection from contacts,[4−42] metal diffusion and quenching of luminescence,[43−45] and modification of metal contacts.[46−48] The method commonly used to fabricate a cathodic metal contact relies on vacuum evaporation of low work function metals or alloys, such as Ca, Mg, Al, Ag, Mg:Ag, and Mg:In.

Like their polymer counterparts, LEDs employing small molecules as emitters have also been of commercial interest.[1,6−10,13,15,17,18,27,49−52] In a recent paper,[53] we reported on single-layer LEDs based on spin-coated solid thin films of Ru(bpy)$_3$(ClO$_4$)$_2$ (bpy = 2,2′-bipyridine) with a cathodic contact achieved by printing of a low melting point alloy such as Ga:In, Ga:Sn, or Bi:In:Pb:Sn. The current−voltage and luminance−voltage plots show a diode-like behavior with a turn-on voltage of 2.3 V. A brightness of up to 3500 cd/m^2 at 4.0 V bias and quantum and power efficiencies of 1.4% and 0.8%, respectively, were realized. The emission spectra showed a maximum at 640−660 nm, and the emission was clearly visible in a lighted room as a bright red emission. In this paper we describe the fabrication and testing of such cells in further detail. Recent work on related cells has also appeared.[54,55] LEDs based on C$_{12}$−Ru(bpy)$_3$(ClO$_4$)$_2$, Ru(phenanthroline)$_3$(ClO$_4$)$_2$, and Os(bpy)$_3$(PF$_6$)$_2$ are also discussed. We also show that this method of making cathodic contacts works with cells based on the more widely used tris(8-hydroxyquinoline)aluminum (Alq$_3$).

Experimental Section

The chemical structures of the major compounds are shown in Figure 1. Commercially available Ru(bpy)$_3$(Cl)$_2$ (Aldrich) was converted to Ru(bpy)$_3$(ClO$_4$)$_2$ by a metathesis reaction with an excess of NaClO$_4$ (Fluka) and then recrystallized twice from

(37) Kim, H.; Gilmore, C. M.; Horwitz, J. S.; Pique, A.; Murata, H.; Kushto, G. P.; Schlaf, R.; Kafafi, Z. H.; Chrisey, D. B. *Appl. Phys. Lett.* **2000**, *76*, 259.
(38) Choi, B.; Yoon, H.; Lee, H. H. *Appl. Phys. Lett.* **2000**, *76*, 412.
(39) Li, F.; Tang, H.; Shinar, J.; Resto, O.; Weisz, S. Z. *Appl. Phys. Lett.* **1997**, *70*, 2741.
(40) Crone, B. K.; Campbell, I. H.; Davids, P. S.; Smith, D. L. *Appl. Phys. Lett.* **1998**, *73*, 3162.
(41) Campbell, I. H.; Davids, P. S.; Smith, D. L.; Barashkov, N. N.; Ferraris, J. P. *Appl. Phys. Lett.* **1998**, *72*, 1863.
(42) Conwell, E. M.; Wu, M. W. *Appl. Phys. Lett.* **1997**, *70*, 1867.
(43) Lee, S. T.; Gao, Z. Q.; Hung, L. S. *Appl. Phys. Lett.* **1999**, *75*, 1404.
(44) Huang, M. B.; McDonald, K.; Keay, J. C.; Wang, Y. Q.; Rosenthal, S. J.; Weller, R. A.; Feldman, L. C. *Appl. Phys. Lett.* **1998**, *73*, 2914.
(45) Choong, V.-E.; Park, Y.; Shivaparan, N.; Tang, C. W.; Gao, Y. *Appl. Phys. Lett.* **1997**, *71*, 1005.
(46) Li, F.; Tang, H.; Anderegg, J.; Shinar, J. *Appl. Phys. Lett.* **1997**, *70*, 1233.
(47) Li, F.; Tang, H.; Shinar, J. *Appl. Phys. Lett.* **1997**, *71*, 2560.
(48) Jabbour, G. E.; Kippelen, B.; Armstrong, N. R.; Peyghambarian, N. *Appl. Phys. Lett.* **1998**, *73*, 1185.

(49) Adachi, C.; Tsutsui, T.; Saito, S. *Appl. Phys. Lett.* **1989**, *55*, 1489.
(50) Burrows, P. E.; Forrest, S. R. *Appl. Phys. Lett.* **1994**, *64*, 2285.
(51) Kido, J.; Kimura, M.; Nagai, K. *Science* **1995**, *267*, 1332.
(52) Strukelj, M.; Jordan, R. H.; Dodabalapur, A. *J. Am. Chem. Soc.* **1996**, *118*, 1213.
(53) Gao, F. G.; Bard, A. J. *J. Am. Chem. Soc.* **2000**, *122*, 7426.
(54) Rudmann, H.; Rubner, M. F. *J. Appl. Phys.* **2001**, *90*, 4338.
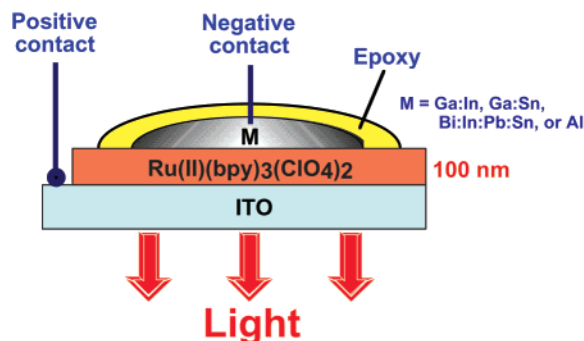(55) Buda, M.; Kalyuzhny, G.; Bard, A. J. *J. Am. Chem. Soc.* **2002**, *124*, 6090−6098.

Figure 2. Structure of the single-layer LED cell.

Figure 3. Optical absorption spectrum of a $Ru(bpy)_3(ClO_4)_2$ thin film on ITO.

an ethanol + acetone (5:1) solution.[56] The perchlorate salt was then dried in a vacuum oven at 125 °C. The synthesis of the derivative C_{12}−$Ru(bpy)_3(ClO_4)_2$ followed the procedure reported previously.[57] $Ru(phenanthroline)_3(ClO_4)_2$ was prepared according to the same procedure,[56] converted from commercially available $Ru(phenanthroline)_3(Cl)_2$ (Aldrich). Os-$(bpy)_3(PF_6)_2$ was synthesized using a procedure described elsewhere.[58] N,N-Bis(3-methylphenyl)-N,N-diphenylbenzidine (TPD) and Alq_3 were purchased from Aldrich. ITO substrates (1.6×2.2 cm^2, Delta Technologies, Ltd., 100 Ω/square except where indicated) were cleaned by sonication in an 80 °C ethanolamine + H_2O (20:80) bath for 20 min, then rinsed and sonicated several times in highly purified Millipore Milli-Q water (18 MΩ cm), and dried in an oven at 95 °C. The structure of a single-layer LED cell is shown in Figure 2. Thin films (about 100 nm thick) of $Ru(bpy)_3(ClO_4)_2$ were spin-coated onto ITO substrates from a 4% (w/v) acetonitrile (Burdick & Jackson, UV grade) solution at room temperature. The $Ru(bpy)_3(ClO_4)_2$ solution was first filtered through a 0.2 μm nylon syringe to remove any large particles. Films were heated in a vacuum oven at 125 °C for at least 8 h. Thin films (ca. 80 nm thick) of C_{12}−$Ru(bpy)_3(ClO_4)_2$ were spin-coated onto ITO sheets from a 4% (w/v) pentanone solution. In some cells, TPD was inserted between ITO and the emitter layer, where it functioned as a hole-transport layer. In these cells, a 0.7% TPD (w/v) xylene solution was used to form a 20 nm thin film by spin coating. Ga:In (75.5:24.5 wt %, mp 15.7 °C) and Ga:Sn (92:8 wt %, mp 20 °C) eutectic cathodes (ca. 3 mm diameter) were printed on the top of the films at room temperature using a syringe and then connected via a thin copper wire inserted into the Ga:In or Ga:Sn contact. Both were then sealed with 5 min epoxy cement (Devcon, Danvers, MA). The light-emitting active area (hereafter referred to as a contact) was about 7 mm^2. Usually four contacts were fabricated for each LED, i.e., for each piece of ITO. In the preparation of the Bi:In:Pb:Sn (49:21:18:12 wt %, mp 58 °C) contact, the alloy was first melted, drawn into a syringe, kept in an oven at 80 °C, and then printed on the top of the film. All eutectics were purchased from Alfa Aesar. For comparison, vacuum-evaporated aluminum contacts were also fabricated. For single-layer LEDs based on Alq_3, a thin film was spin-coated onto ITO from a saturated Alq_3 pyridine solution. Then, the same procedure as that used in making a $Ru(bpy)_3(ClO_4)_2$ device was followed.

Spin coating of the thin film was carried out by a Headway model E101 spinner. All LEDs were fabricated in a laminarflow hood under ambient conditions. Current−voltage, luminance−voltage, current−time, and luminance−time characteristics were measured at room temperature with an Autolab GPES (General Purpose Electrochemical System, ECO Chemie BV, The Netherlands) and a Newport Optical Power Meter (model 1830-c) equipped with a 818-UV semiconductor detector (1 cm^2) connected to the Autolab GPES via its auxiliary second ADC signal i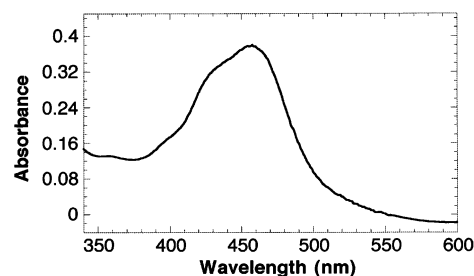nput ports. The reference and counter electrode leads of the Autolab GPES potentiostat were connected together to obtain the desired voltage at the LED electrodes. The emission spectra were measured with a model CH210 CCD camera equipped with a monochromator and cooled to −125 °C. The optical absorption spectra were measured with a Milton Roy (San Leandro, CA) Spectronic 3000 diode array UV−vis spectrophotometer. Digital photographs and optical microscopy were recorded with an Olympus BH-2 microscope equipped with a Pixera digital visual system. Digital fluorescence microscopy CCD pictures were taken with a confocal optical microscope (Olympus SZX12) equipped with 470 nm (excitation) and 515 nm long-pass (emission) filters. Atomic force microscopy (AFM) images were captured using a Nanoscope III with an AFM 619E-Z head (Digital Instruments, Santa Barbara, CA) using a SiN tip in the contact mode. Vacuum evaporation of Al contacts was carried out with an evaporator from Vacuum Engineering Co., Inc.

Results and Discussion

$Ru(bpy)_3(ClO_4)_2$ Thin Film Characteristics. Figure 3 is the optical absorption spectrum of a $Ru(bpy)_3(ClO_4)_2$ thin film on ITO, indicating a maximum absorption at 455 nm. The optical microscope image of the $Ru(bpy)_3(ClO_4)_2$ thin film in Figure SI 1 shows a relatively smooth and uniform surface. The AFM image of the film topography on ITO in Figure SI 2 (upper) shows a roughness of about 40 nm. A 100 nm thin film thickness was determined by making a light scratch on the surface and measuring the AFM line profile across it [Figure SI 2 (lower)].

A transmission electron microscope image of the $Ru(bpy)_3(ClO_4)_2$ films [Figure SI 3 (upper)] suggests that the films are amorphous [also confirmed by the X-ray diffraction pattern of the film, in Figure SI 2 (lower)]. The $Ru(bpy)_3(ClO_4)_2$ films are solid, i.e., contain no or trace solvent, as can be seen from the differential thermal analysis of the thin film in Figure SI 4.

$Ru(bpy)_3(ClO_4)_2$-Based LEDs. Figure 4 (upper) is a photograph showing emission from two contacts of a single-layer LED with the structure (+)ITO/$Ru(bpy)_3$-$(ClO_4)_2$/Ga:In(−) at a voltage bias of 3.0 V. Unless otherwise mentioned, the ITO contact in experiments was positive, and this will be termed the forward bias direction. The bright red emission was clearly visible in a lighted room. A similar emission was obtained for the LEDs using Ga:Sn, Bi:In:Pb:Sn, or Al as the contact. Figure 4 (lower) shows the emission spectrum of the LED using Ga:In as the cathodic contact, indicating a maximum emission at 660 nm, a half-maximum width of 140 nm, and a relatively long tail toward the red. There was, at most, a very small (ca. 10 nm) blue shift when the voltage bias increased from 3.1 to 9.4 V. This emission spectrum was essentially the same at the photoluminescence spectrum of the thin film.

(56) McCord, P.; Bard, A. J. *J. Electroanal. Chem.* **1991**, *318*, 91.
(57) Sprintschnik, G.; Sprintschnik, H. W.; Kirsch, P. P.; Whitten, D. G. *J. Am. Chem. Soc.* **1977**, *99*, 4947.
(58) Gaudiello, J. G.; Bradley, P. G.; Norton, K. A.; Woodruff, W. H.; Bard, A. J. *Inorg. Chem.* **1984**, *23*, 3.
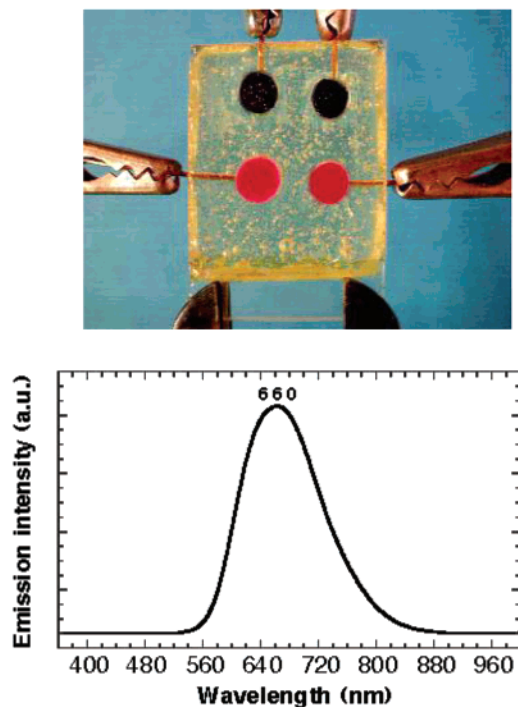
Figure 4. Photograph (upper) showing red emission from two contacts of a single-layer LED ITO/Ru(bpy)$_3$(ClO$_4$)$_2$/Ga:In. Emission spectrum of a single-layer LED ITO/Ru(bpy)$_3$(ClO$_4$)$_2$/Ga:In (lower).
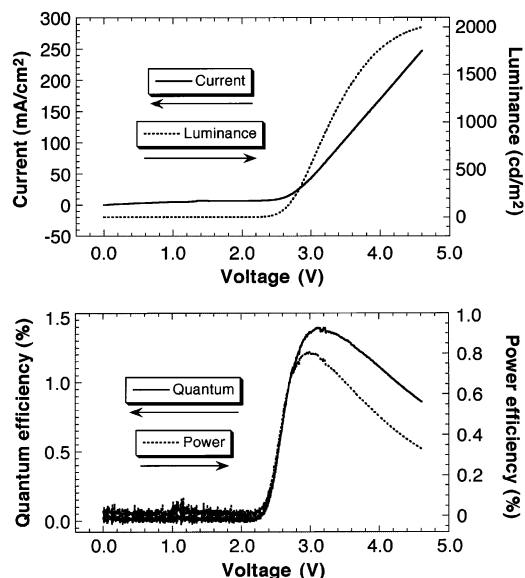

Figure 5. Current−voltage and luminance−voltage plots of a single-layer LED (+)ITO/Ru(bpy)$_3$(ClO$_4$)$_2$/Ga:In(−) (upper). The voltage scan rate was 0.05 V/s. External quantum efficiency and power efficiency as a function of the voltage bias (lower).

Figure 5 (upper) shows the current−voltage and luminance−voltage plots of a single-layer LED (+)ITO/Ru(bpy)$_3$(ClO$_4$)$_2$/Ga:In(−) (forward bias). The LED showed a turn-on voltage of about 2.3 V for both current and emission. The device reached a luminance level of 500 cd/m^2 at 3 V and a maximum luminance of 2000 cd/m^2 at about 4.5 V. Plots of external quantum efficiency and power efficiency as a function of voltage bias in Figure 5 (lower) show that with a voltage bias above 2.3 V the quantum efficiency and power efficiency rapidly increase
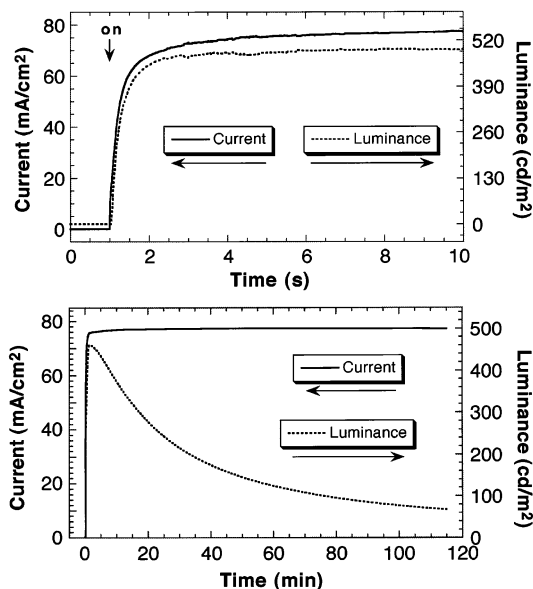
Figure 6. Current and luminance transient curves upon application of a 3.0 V voltage bias for the LED ITO/Ru(bpy)$_3$-(ClO$_4$)$_2$/Ga:In (upper). Same but over 2 h (lower).

with voltage. At about 3.0 V, they reached maximum values of 1.4% and 0.8% (equivalent to about 1−2 lm/W), respectively, and then slowly decreased with a further increase in voltage. Results from a group of LEDs prepared by the same procedure showed considerable variations in an external quantum efficiency ranging from 0.4% to 1.8% and power efficiencies from 0.2% to 1.2% [Figure SI 5 (upper and lower left)].

Figure 6 (upper) shows the current and luminance curves vs time upon application of a 3.0 V voltage step. The time delay for the rise of the emission was only about 0.02 s, with about 1−2 s needed to reach the maximum luminance output. Variations in delay time for maximum emission were observed among the devices, ranging up to 1−5 s. The emission began to decrease soon after it reached the maximum, as shown by a time course of both the current and luminance [Figure 6 (lower)]. Typically, the luminance declined by more than 50% in 1 h. The intensity of the emitted light continued to decrease over several hours and then maintained a nearly steady level. After 5 h the emission was still visible with an intensity of about 20 cd/m^2. The higher the applied voltage, the shorter the delay time for the emission rise and the shorter the time for emission to decay to half its initial value. In contrast to the rapid decrease of the luminance, the current fell slightly, if at all, during operation.

Influence of a TPD Hole-Transport Layer. For comparison, we also investigated LEDs with TPD as a hole transporter inserted between the ITO and the Ru(bpy)$_3$(ClO$_4$)$_2$ layer: (+)ITO/TPD/Ru(bpy)$_3$(ClO$_4$)$_2$/Ga:In(−). Results of a group of 20 bilayer LEDs showed about the same performance as that revealed in Figure SI 5 (right). Thus, a TPD layer did not significantly improve the performance of the LED cells in terms of brightness or lifetime. The performance appears to be governed largely by the quality of the Ru(bpy)$_3$(ClO$_4$)$_2$ thin films formed on ITO substrates.

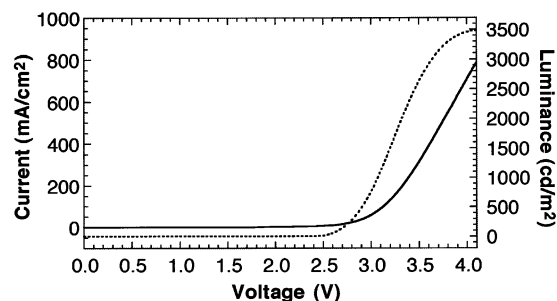**Influence of ITO Resistivity.** We typically used ITO with a resistivity of 100 Ω/square. To understand

Figure 7. Current−voltage and luminance−voltage plots of a single-layer LED using 10 Ω/square ITO as the substrate, i.e., ITO (10 Ω/square)/Ru(bpy)$_3$(ClO$_4$)$_2$/Ga:In. The voltage scan rate was 0.05 V/s.
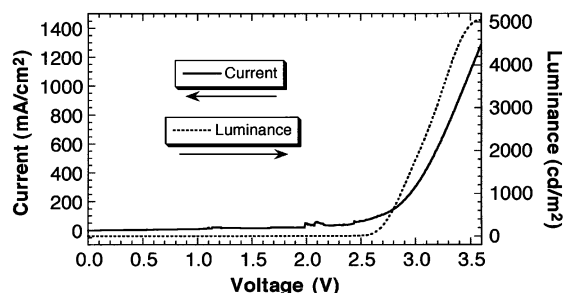

Figure 8. Current−voltage and luminance−voltage plots of a single-layer LED with a semitransparent gold layer inserted between ITO and the emitter layer, i.e., ITO/Au/Ru(bpy)$_3$(ClO$_4$)$_2$/Ga:In. The voltage scan rate was 0.05 V/s.

the influence of ITO resistivity on the performance of LEDs, we tested similar LEDs fabricated by the same process mentioned above but using 10 Ω/square ITOs. Figure 7 shows the current−voltage and luminance−voltage plots of a single-layer LED with the structure of (+)ITO (10 Ω/square)/Ru(bpy)$_3$(ClO$_4$)$_2$/Ga:In(−). The LED showed current−voltage and luminance−voltage behavior very similar to those with 100 Ω/square ITO, though with a greater current density and hence emission, at a relatively low field, reaching 3500 cd/m^2 at 4.0 V voltage bias. Quantum and power efficiencies showed no improvement over those obtained using 100 Ω/square ITO. For LEDs using more heavily In-doped 10 Ω/square ITO, holes were injected more efficiently from the ITO into the Ru(bpy)$_3$(ClO$_4$)$_2$ layer, resulting in a significant increase of the intensities of current (injected holes from the anode and electrons from the cathode) and emission (by recombination of holes and electrons).

Figure 8 indicates that a much higher current density (hence a greater emission intensity) was obtained with an LED (+)ITO/Au/Ru(bpy)$_3$(ClO$_4$)$_2$/Ga:Sn(−), with about a 10 nm semitransparent gold film inserted between the ITO and the Ru(bpy)$_3$(ClO$_4$)$_2$ film. For this device a luminance as high as 5000 cd/m^2 at 3.5 V was realized. Gold, in all probability, is a better hole injecting material than ITO. As a result, at the same field, more holes were injected from the ITO/Au side into the Ru(bpy)$_3$(ClO$_4$)$_2$ film and, hence, more holes and electrons recombined, resulting in an enormous increase in both current and emission. However, as with LEDs using different ITOs, there was no significant difference in lifetime between the devices with an Au film inserted between the ITO and the Ru(bpy)$_3$(ClO$_4$)$_2$ film and those without one.

Different Cathodic Contacts. In addition to Ga:In, we used other low melting point alloys, Ga:Sn and Bi:In:Pt:Sn, as cathodic contacts. Figure SI 6 is a photograph showing emission from two contacts of a single-layer LED with the structure ITO/Ru(bpy)$_3$(ClO$_4$)$_2$/Ga:Sn(−) at 3.0 V. The bright red emission was clearly visible in a lighted room. Figure SI 6 (lower) is a photograph showing emission from two contacts of a single-layer LED ITO/Ru(bpy)$_3$(ClO$_4$)$_2$/Bi:In:Pt:Sn at 3.0 V. Ru(bpy)$_3$(ClO$_4$)$_2$-based LEDs using Ga:In, Ga:Sn, and Bi:In:Pt:Sn as cathodic contacts show very similar performances in current−voltage and luminance−voltage behavior, turn-on voltage, and emission spectra. Evaporated Al and printed Hg were also used as cathodic contacts, and visible red emissions were obtained for those LEDs using Al and Hg contacts.

Mechanism of Electroluminescence (EL). We present a detailed model of the EL process in these films elsewhere.[55] In brief, the EL mechanism in the solid state is proposed to occur by an electrochemical process, similar to the electrogenerated chemiluminescence (ECL) mechanism in solution arising from the annihilation of Ru(bpy)$_3$$^{3+}$ (holes in the solid state residing mainly on the Ru) and Ru(bpy)$_3$$^+$ (electrons in the solid state residing mainly on the bipyridines). As described elsewhere,[55] establishment of the needed fields at both contacts requires some mobility of the ClO$_4$$^−$ with electrons injected from the cathode and holes from the anode. Hopping of holes and electrons, between Ru(bpy)$_3$$^{2+}$ sites, forms Ru^{III}(bpy)$_3$$^{3+}$ and Ru^{II}(bpy)$_2$(bpy$^−$)$^+$ sites, and where these meet in the film, the annihilation reaction produces Ru^{II}(bpy)$_3$$^{2+*}$. The balance between electron injection and hole injection governs the quantum efficiency; excess electrons or holes migrate to the opposite electrode without undergoing the annihilation reaction.

Mechanism of Emission Decay. An important problem with the possible application of Ru(bpy)$_3$(ClO$_4$)$_2$-based LEDs is their relatively short lifetime (on the order of a few hours), and experiments were undertaken to understand the emission decay mechanism. Because the results discussed above were obtained with LEDs fabricated and tested under ambient conditions, we tested LEDs, formed by spin coating in the ambient, in a dry Ar atmosphere but found no significant improvement in lifetime. We also changed anode materials from ITO to ATO (antimony-doped tin oxide) and Au, again noting no improvement in emission lifetime. Furthermore, we found that LEDs using various cathodic contacts, such as Ga:In, Ga:Sn, Bi:In:Pt:Sn, Al, and Hg cathode contacts, showed similar emission decays.

We also studied the effect of cell operation lifetime on the photoluminescence of the film. Figure SI 7 is a photoluminescence confocal microscope CCD picture of a four-contact LED (+)ITO/Ru(bpy)$_3$(ClO$_4$)$_2$/Ga:Sn(−). The contact at the upper right corner, operated for 100 h at 4.5 V bias, showed no or very weak fluorescence, while the other contacts that remained at open circuit showed intense red-orange emission. The emission intensity decreased with operation time and was noticeably decreased after 1 h of operation and almost completely quenched after 72 h (Figure SI 8).
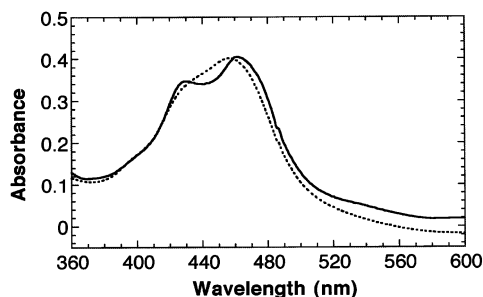
Figure 9. Optical absorption spectrum of an ITO/Ru(bpy)$_3$-(ClO$_4$)$_2$ film before operation (dotted line). In the same area, a Hg contact was made, and a 8.0 V voltage bias was added for 5 h, then the Hg contact was removed, and an optical absorption spectrum of the ITO/Ru(bpy)$_3$(ClO$_4$)$_2$ film in the same area was measured (solid line).

The Ru(bpy)$_3$(ClO$_4$)$_2$ compound itself is thermally stable and does not appear to decompose after 100 h of operation. Figure 9 (dotted line) shows the optical absorption spectrum of a fresh ITO/Ru(bpy)$_3$(ClO$_4$)$_2$ film before operation. A Hg contact was made to the same ITO/Ru(bpy)$_3$(ClO$_4$)$_2$ film and an 8.0 V voltage bias was applied, resulting in a bright red emission which decayed with time. After 5 h of operation, the Hg contact was removed and the optical absorption spectrum of the ITO/Ru(bpy)$_3$(ClO$_4$)$_2$ film in the same region was measured again. This is shown in Figure 9 (solid line). No significant decrease in the absorbance of Ru(bpy)$_3$(ClO$_4$)$_2$ was observed. However, the optical absorption spectrum of the film after operation showed two peaks.

The results suggest the buildup of a quencher during operation. It is also possible that migration of metal ions from the contacts into the film and impurities in the film play a role in the process. Further experiments along these lines are currently underway.

C$_{12}$−Ru(bpy)$_3$(ClO$_4$)$_2$ and Ru(phenanthroline)$_3$-(ClO$_4$)$_2$. We also fabricated LEDs with a spin-coated single layer of C$_{12}$−Ru(bpy)$_3$(ClO$_4$)$_2$ or Ru(phenanthroline)$_3$(ClO$_4$)$_2$ as the emitter and printed Ga:Sn as the cathodic contact. Although a clearly visible red emission was generated for both LEDs, their luminance and efficiencies are much less than those using Ru(bpy)$_3$-(ClO$_4$)$_2$ as the emitter. The emission spectra of two LEDs using C$_{12}$−Ru(bpy)$_3$(ClO$_4$)$_2$ and Ru(phenanthroline)$_3$-(ClO$_4$)$_2$, respectively, are given in Figures SI 9 and SI 10.

Os(bpy)$_3$(PF$_6$)$_2$. Red emission is seen from the single-layer LED (+)ITO/Os(bpy)$_3$(PF$_6$)$_2$/Ga:Sn(−) (see Figure SI 11). The lower part of Figure SI 11 shows the emission spectrum of this LED, with a maximum at about 700 nm. Although the intensity and efficiency of these cells was also much smaller than those obtained using Ru(bpy)$_3$(ClO$_4$)$_2$ as the emitter, the emission lifetime was much longer. Figure 10 shows the time course of the current and luminescence.

Alq$_3$. Alq$_3$ has been extensively studied as a component of LEDs. These cells behave as typical semiconductor LEDs and utilize low work function cathodes, like Ca. Low melting point alloys as cathodic contacts have not been investigated. To see if such a cathode would
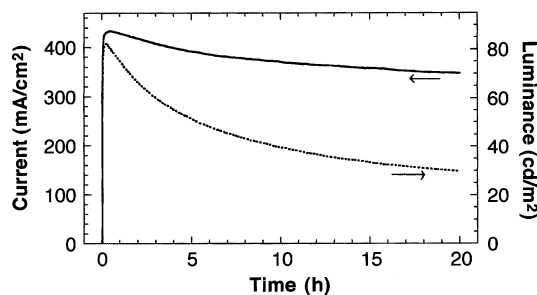

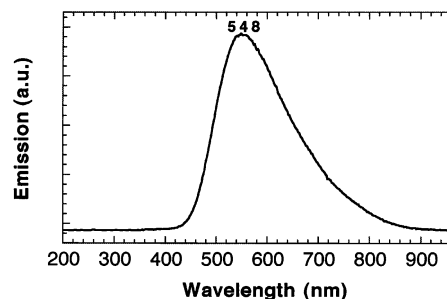**Figure 10.** Current and luminance curves against time upon application of 5.0 V voltage bias for the LED ITO/Os(bpy)$_3$-(PF$_6$)$_2$/Ga:Sn.

Figure 11. Emission spectrum of a single-layer LED ITO/Alq$_3$/Ga:Sn.

work, a single-layer LED, (+)ITO/Alq$_3$/Ga:Sn(−), was constructed. This emitted visible green-yellow light upon the application of a forward voltage bias. Its emission spectrum, with a maximum at 550 nm, is shown in Figure 11. Printed low melting point alloys may, therefore, prove useful in LEDs employing small molecules, or perhaps polymers, as light emitters.

Conclusions

We have demonstrated high brightness (3500 cd/m^2 at 4.0 V) and low voltage driven LEDs (turn-on voltage of 2.3 V) based on an amorphous film of Ru(bpy)$_3$(ClO$_4$)$_2$ as the emitter and using printed low melting point alloys such as Ga:In, Ga:Sn, and Bi:In:Pb:Sn as cathodic contacts. The relatively short emission lifetime (hours) is probably due to quenching of the Ru(bpy)$_3$(ClO$_4$)$_2$ excited state by species formed in the film during operation.

Supporting Information Available: This material is available free of charge via the Internet at http://pubs.acs.org.

CM020117H

Supporting Information Figure Captions

Figure SI 1   Optical microscope image of a $Ru(bpy)_3(ClO_4)_2$ thin film on ITO. The width of the image is 50 μm.

Figure SI 2   AFM topograph of a $Ru(bpy)_3(ClO_4)_2$ thin film on ITO (upper). An AFM line profile of the $Ru(bpy)_3(ClO_4)_2$ thin film surface with a scratch, showing a thickness of 100 nm (lower).

Figure SI 3   Transmission electron microscope image of the $Ru(bpy)_3(ClO_4)_2$ thin film (upper). X-ray diffraction pattern of the $Ru(bpy)_3(ClO_4)_2$ thin film (lower).

Figure SI 4   Thermal analysis of the $Ru(bpy)_3(ClO_4)_2$ thin film. Sample was held at 50.00 °C for 1 min, heated from 50.00 °C to 200.00 °C at 10.00 °C/min.

Figure SI 5   External quantum efficiencies (upper) and power efficiencies (lower) of a group of single-layer LED $ITO/Ru(bpy)_3(ClO_4)_2/Ga$:In (left) and double-layer LED $ITO/TPD/Ru(bpy)_3(ClO_4)_2/Ga$:In (right).

Figure SI 6   Photograph (upper) showing red emission from two contacts of a single-layer LED $ITO/Ru(bpy)_3(ClO_4)_2/Ga$:Sn. Photograph (lower) showing red emission from two contacts of a single-layer LED $ITO/Ru(bpy)_3(ClO_4)_2/Bi$:In:Pt:Sn.

Figure SI 7   Photoluminescence confocal microscope CCD pictures of an LED $ITO/Ru(bpy)_3(ClO_4)_2/Ga$:Sn. The contact at the upper right corner had been operated for 100 h at 4.5 V bias, showing no or very weak fluorescence. The remaining three contacts, held at open circuit, show intense red fluorescence. Excitation 470 nm, emission 515 nm LP, magnification 8, exposure time 1 s.

Figure SI 8 Photoluminescence confocal microscope CCD pictures of a contact of an LED ITO/Ru(bpy)$_3$(ClO$_4$)$_2$/Ga:Sn, (a) before operation, showing intense red fluorescence, and after operation at 4.5 V voltage bias for (b) 1 h, (c) 20 h, and (d) 72 h, showing that the fluorescence intensity decreased with operation time. Excitation 470 nm, emission 515 nm LP, magnification 50, exposure time 1/8 s.
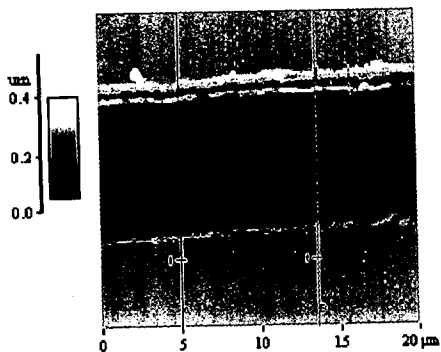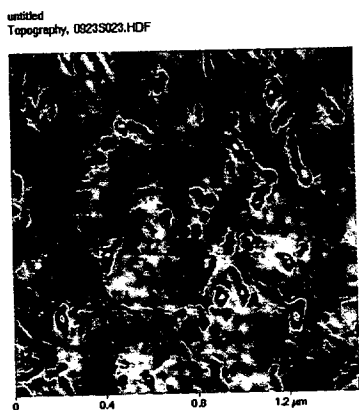
Figure SI 9 Emission spectrum of a single-layer LED ITO/C$_{12}$- Ru(bpy)$_3$(ClO$_4$)$_2$/Ga:Sn.

Figure SI 10 Emission spectrum of a single-layer LED TO/Ru(phenanthroline)$_3$(ClO$_4$)$_2$/Ga:Sn.

Figure SI 11 Photograph showing red emission from two contacts of a single-layer LED ITO/Os(bpy)$_3$(PF$_6$)$_2$/Ga:Sn.

SI Figure 1

untitled
Topography, 0923S023.HDF
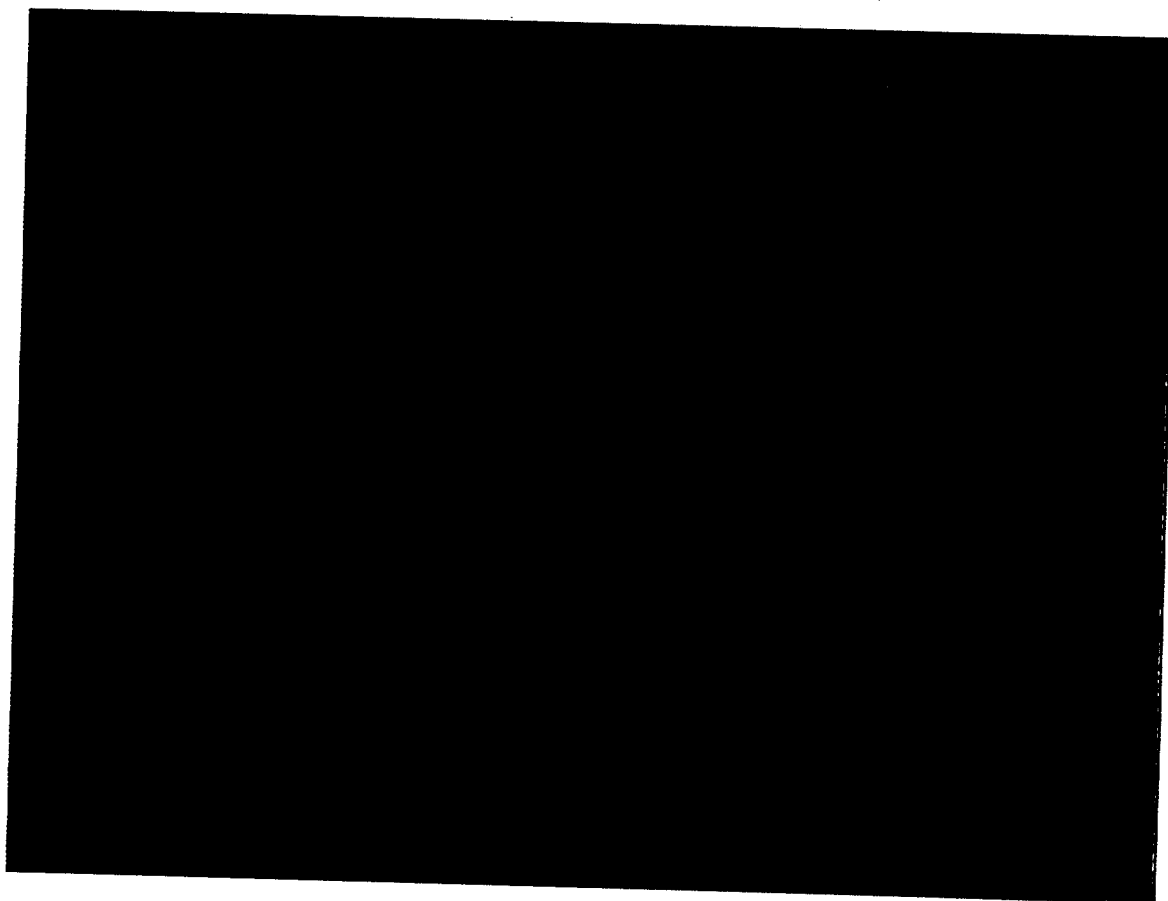
Line Profile Measurements

Topography, 0922S00B.HDF

Height Profile [A]

Height Profile [B]
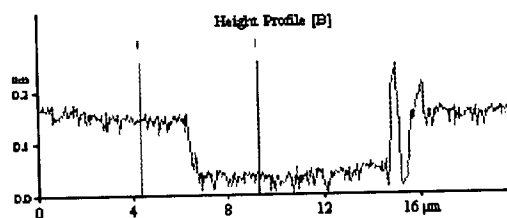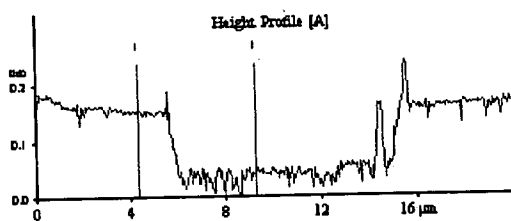
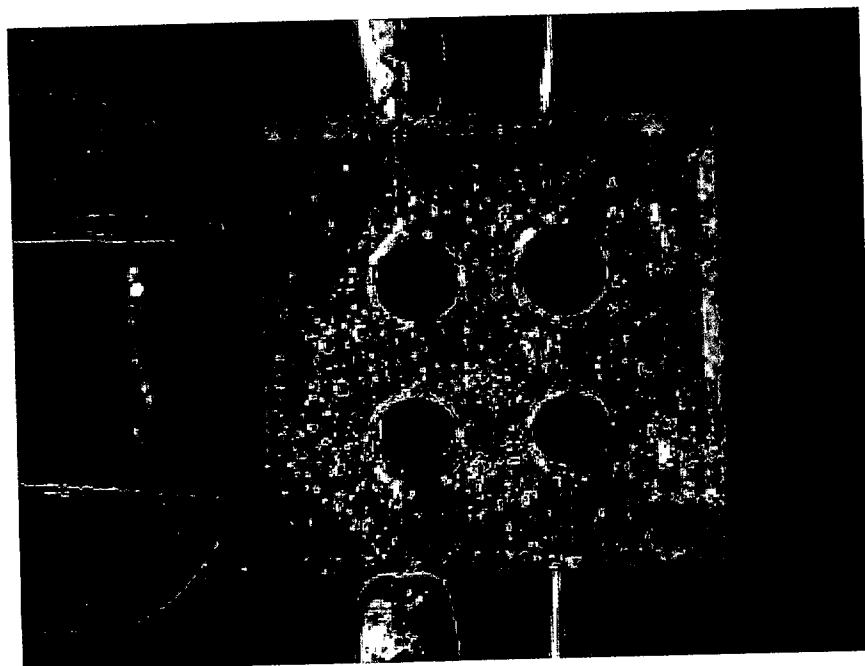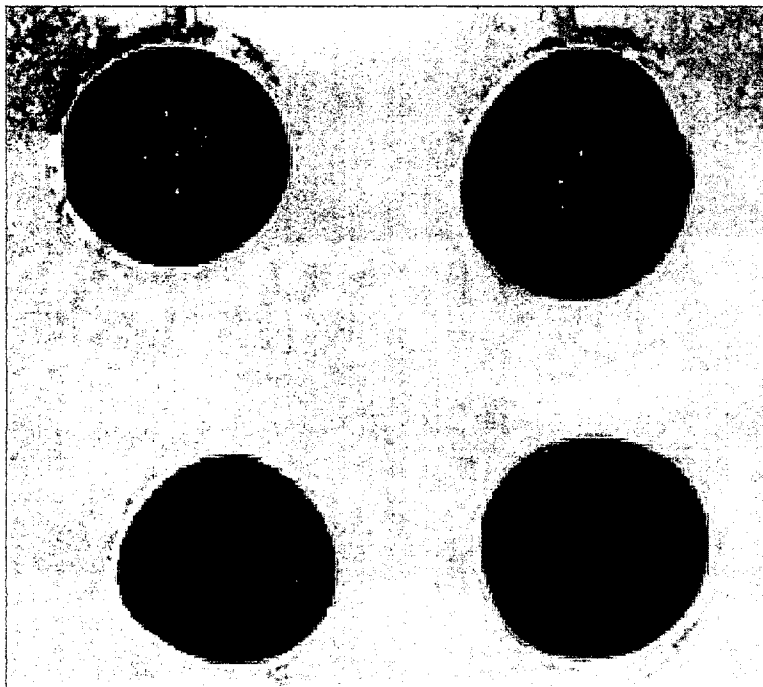| Line	Height	Distance
[A]	1: 0.104 um	1: 4.89 um
[B]	1: 0.109 um	1: 4.89 um

SI Figure 2 Upper and Lower
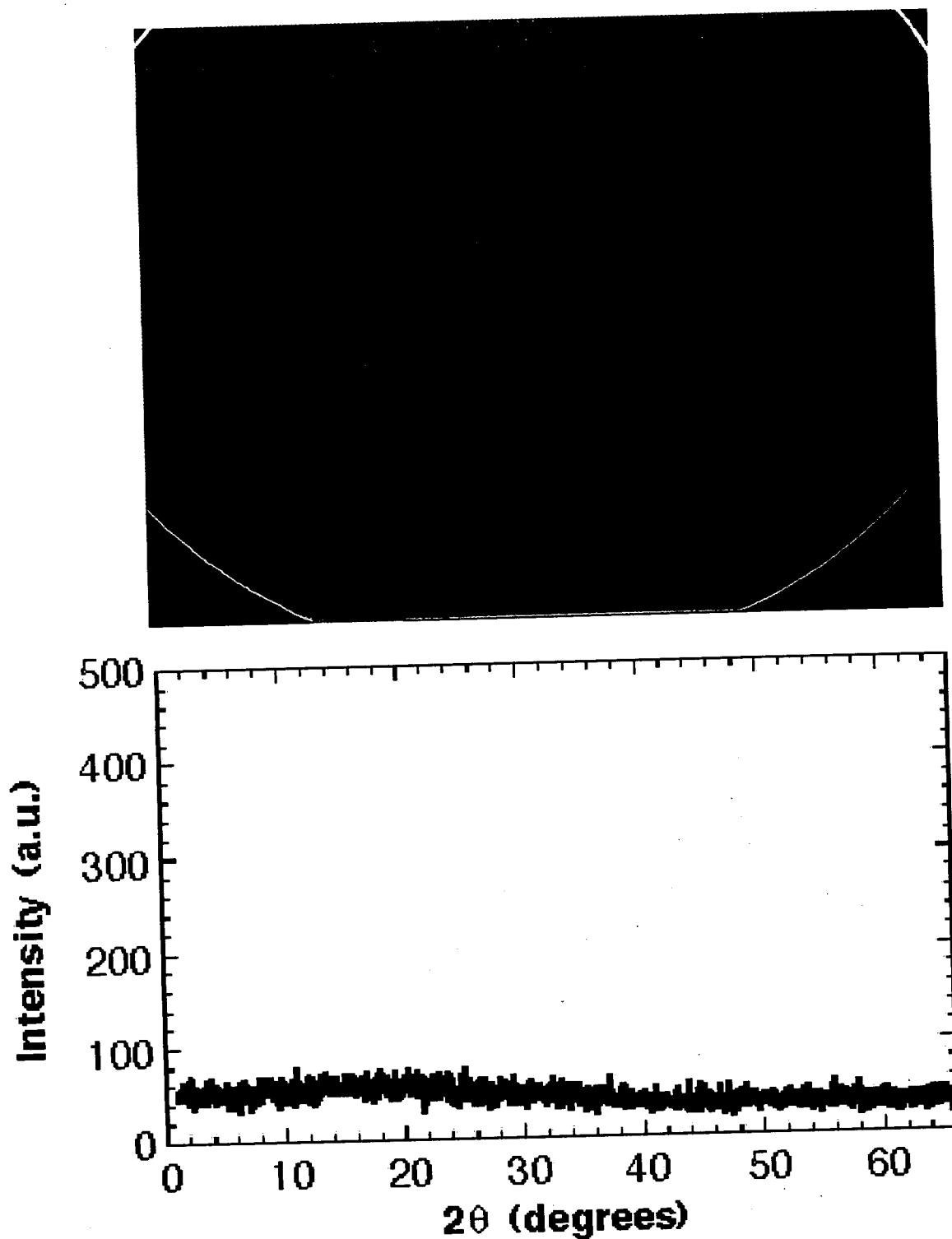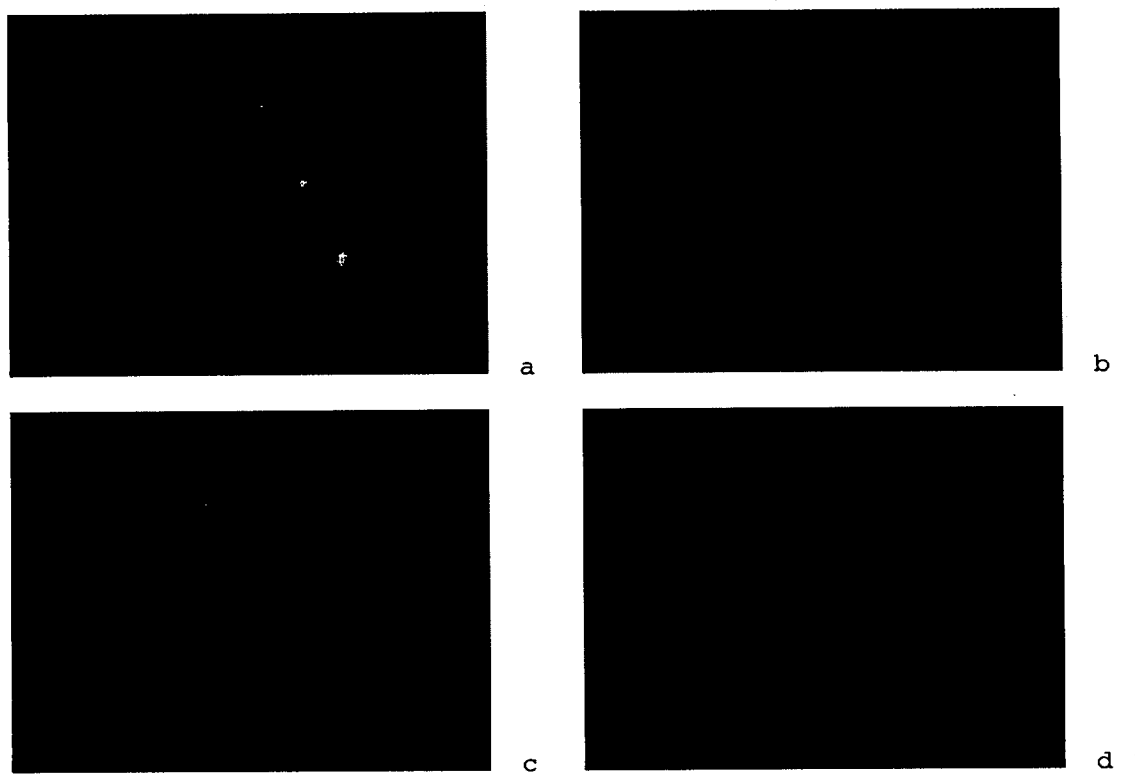
SI Figure 3 Upper and Lower
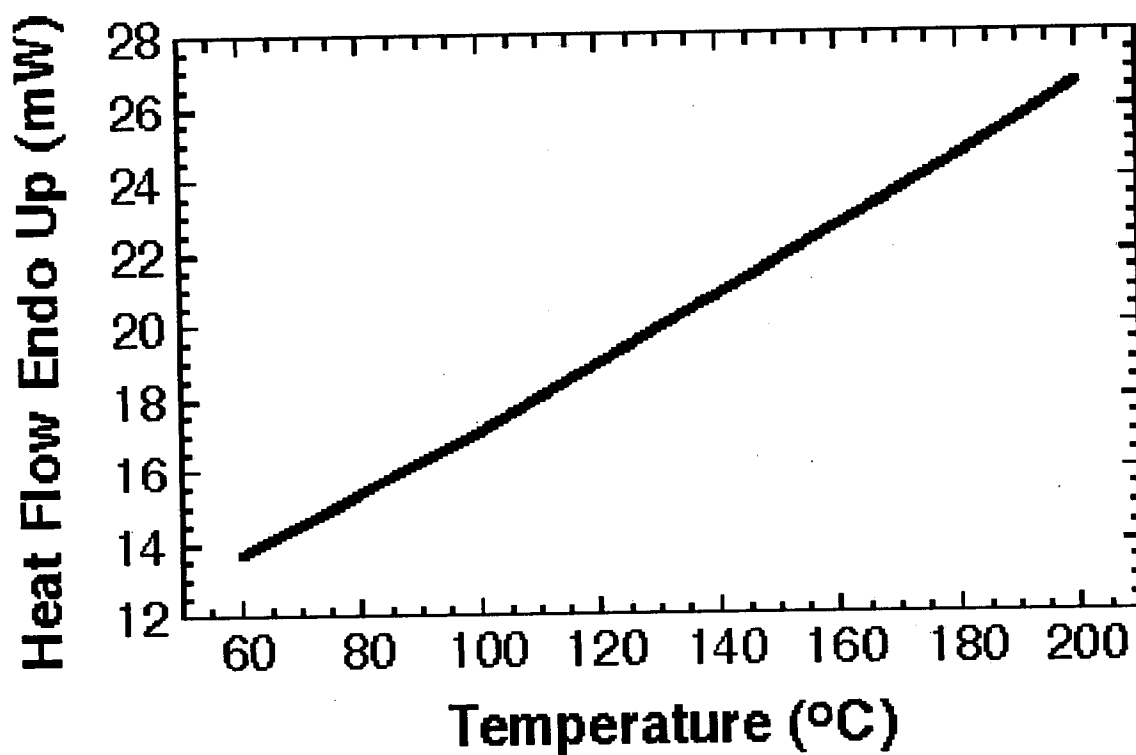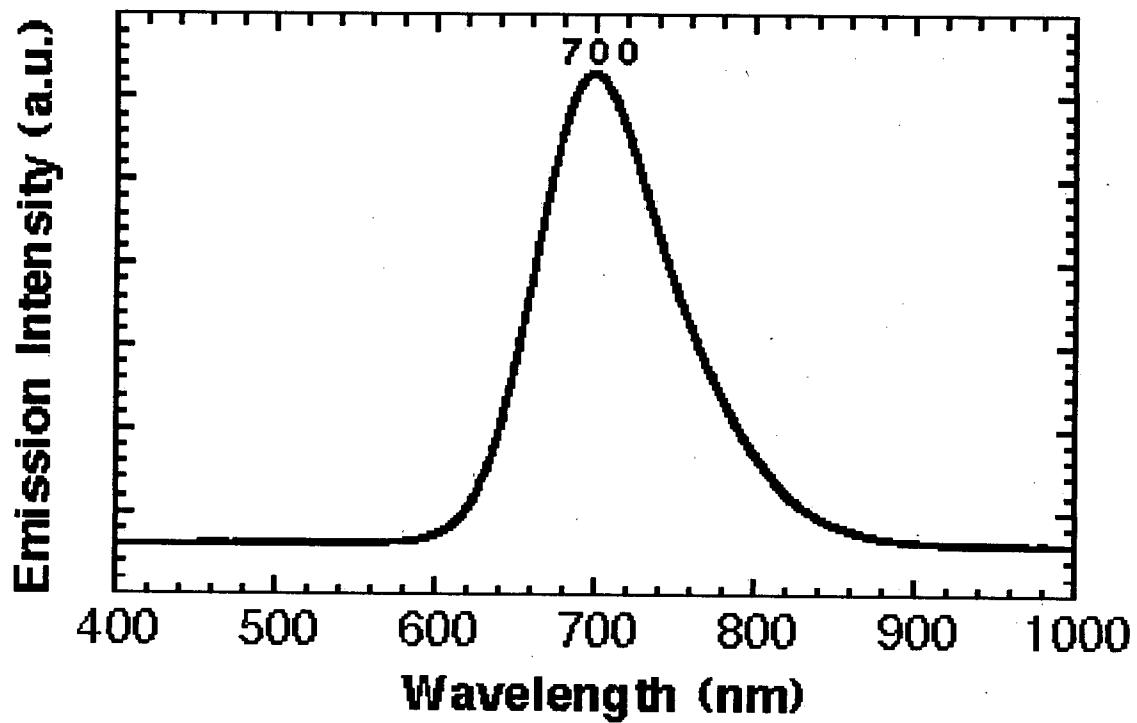
SI Figure 4
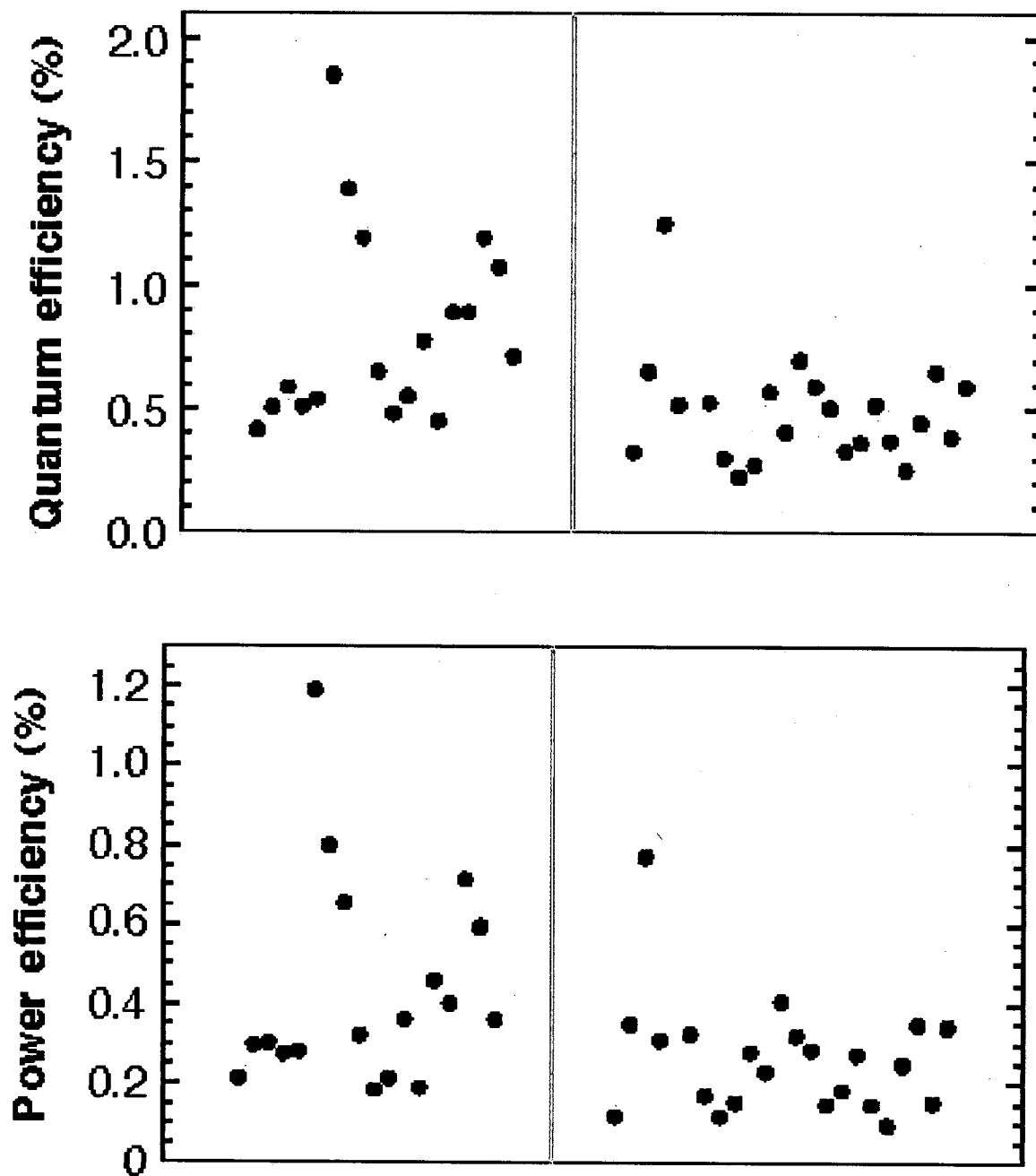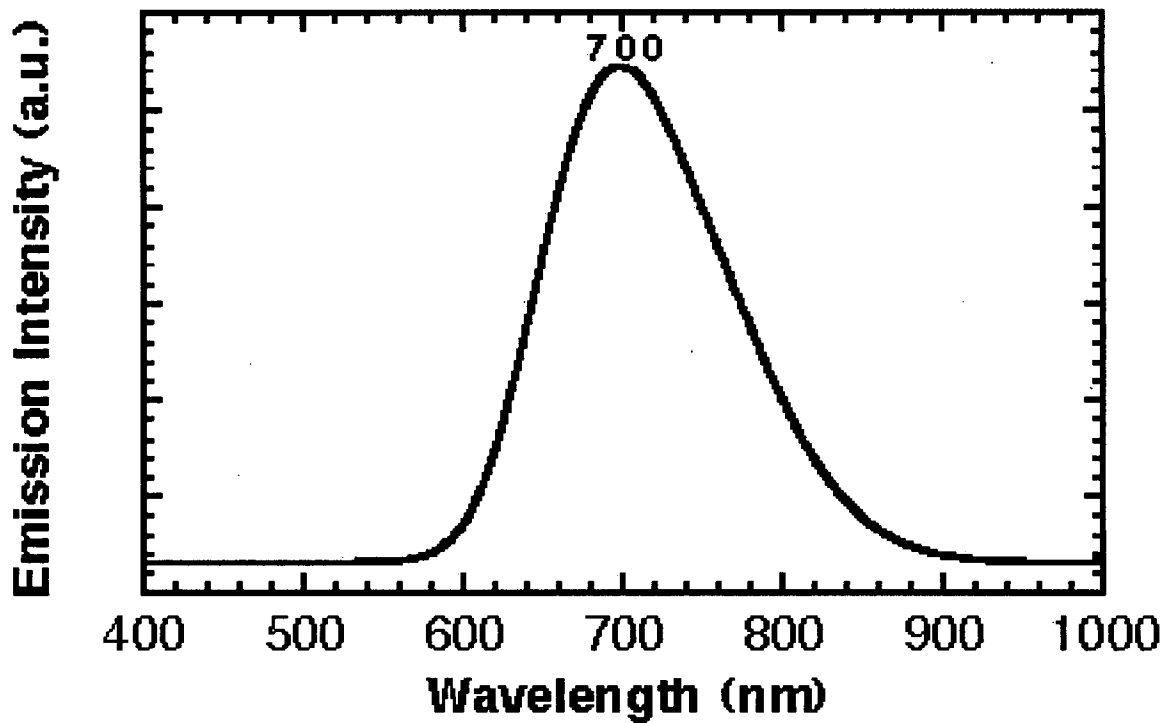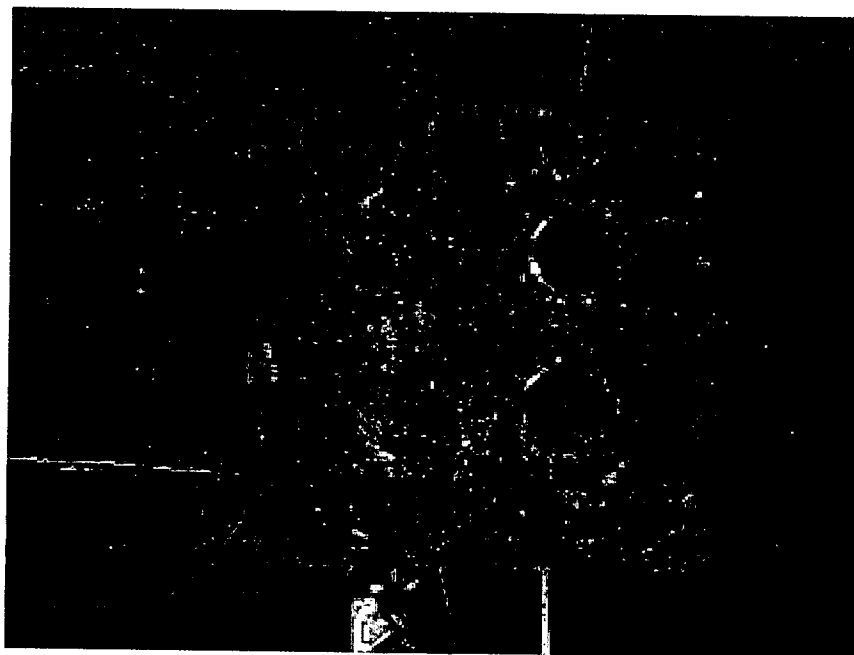
SI Figure 5 Upper and Lower
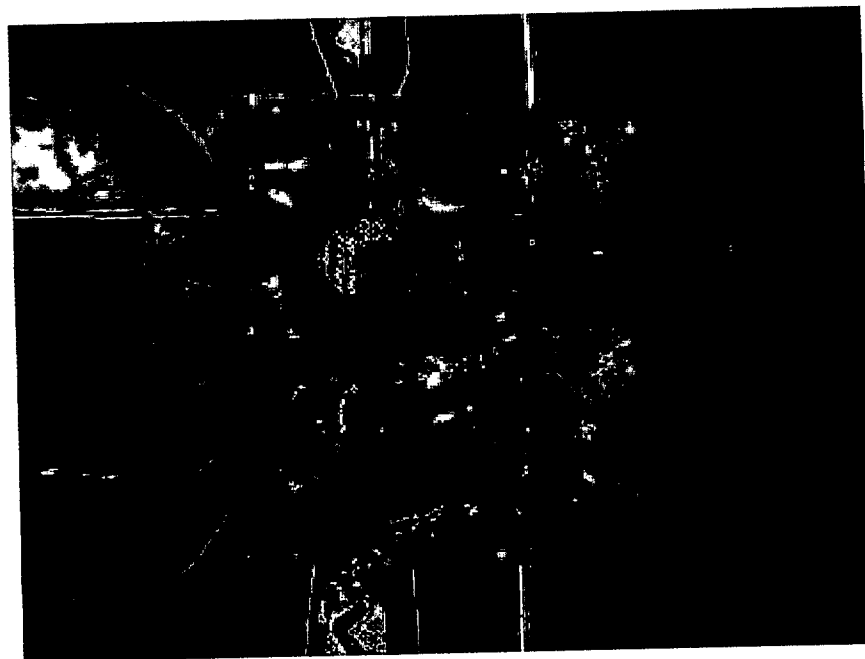
SI Figure 6 Upper and Lower

SI Figure 7

SI Figure 8a-d

SI Figure 9

SI Figure 10

SI Figure 11